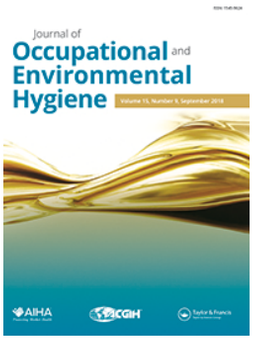

Journal of Occupational and Environmental Hygiene

ISSN: 1545-9624 (Print) 1545-9632 (Online) Journal homepage: http://www.tandfonline.com/loi/uoeh20

Characterization of paint dust aerosol generated from mechanical abrasion of TiO_2-containing paints

Adam W. Nored, Marie-Cecile G. Chalbot & Ilias G. Kavouras

To cite this article: Adam W. Nored, Marie-Cecile G. Chalbot & Ilias G. Kavouras (2018) Characterization of paint dust aerosol generated from mechanical abrasion of TiO_2-containing paints, Journal of Occupational and Environmental Hygiene, 15:9, 629-640, DOI: 10.1080/15459624.2018.1484126

To link to this article: https://doi.org/10.1080/15459624.2018.1484126

JOURNAL OF OCCUPATIONAL AND ENVIRONMENTAL HYGIENE
2018, VOL. 15, NO. 9, 629–640
https://doi.org/10.1080/15459624.2018.1484126

Taylor & Francis
Taylor & Francis Group

Characterization of paint dust aerosol generated from mechanical abrasion of TiO_2-containing paints

Adam W. Nored[a], Marie-Cecile G. Chalbot[b], and Ilias G. Kavouras[c]

[a]Interdisciplinary Engineering Program, University of Alabama at Birmingham, Birmingham, Alabama; [b]School of Arts and Sciences, College of New Rochelle, New Rochelle, New York; [c]Department of Environmental, Occupational and Geospatial Health Sciences, City University of New York, New York, New York

ABSTRACT

The purpose of the study was to determine the potential for release of titanium dioxide nanoparticles in paint dust. The coatings aerosol resuspension system was developed and used for testing the generation and physical, chemical, and morphological properties of paint dust particles from mechanical abrasion (i.e., sanding) of coated wood surfaces. The paint dust emissions from bare and coated wood surfaces with multiple coatings using variable sandpaper grits were evaluated. Substantially higher particle number concentrations were measured for paint dust containing particles in the nano range (particles with aerodynamic diameter less than 100 nm) than those measured for wood dust. The variability of particle number concentration and size distribution of paint dust derived under different conditions indicated that considerable quantities of nanoparticles might be released from mechanical abrasion of painted surfaces that may induce unhealthy exposure conditions. Moreover, spectroscopic and microscopic analysis identified the presence of paint and wood components in paint dust, including titanium dioxide agglomerates that were originally embedded in the paint. The agglomerates were mostly attached to particles with sizes $<$100 nm, enabling them to potentially penetrate into the lower respiratory tract. These results demonstrated that the paint dust exposure generation system can provide qualitative and quantitative information on particle emissions and the abundance of nanoparticles from paint sanding in realistic conditions and they may be used to assess occupational and environmental exposures and risks. Furthermore, the prevalence of titanium dioxide nanoparticles in paint dust highlights the potential for exposures of painters and other occupational groups to hazardous paint dust and the need for protective devices and strategies aiming to reduce exposures to nanoparticles.

KEYWORDS

Nanoparticles; pigments; sanding; scanning electron microscopy; spectroscopy

Introduction

Metals and metal oxides nanoparticles (i.e., particles whose size, shape, and chemical content are manufactured in the nano-scale) have been integrated as free powders, stabilized particles in suspensions or mixed into paint batches and granulates.[1] They improve the properties and functionality of paints such as coloring, integrity, thermal insulation, bactericidal activity, fire retardant, and self-cleaning.[2–7] Those typically used in coatings include titanium dioxide (TiO_2), silicon dioxide (SiO_2), silver (Ag), zinc oxide (ZnO), and aluminum oxides (Al_2O_3).[8] Inhaled pristine nano-metals and metal oxides affect the lung, but are also cleared into circulatory systems, lymphatic system, nervous system, gastrointestinal tract, and cross the blood/brain barrier.[9–13] They are shown to induce fibrosis, emphysema, and tumors in the respiratory tract, lymphocytes damage, thrombosis, cardiovascular, and neurodegenerative diseases.[14–18]

Construction and maintenance painting workers are exposed to a large variety of substances in paint and paint dust. There are at least 215,000 painters in this sector excluding part-time and undocumented workers who may comprise a significant fraction of the construction workforce.[19] Painters are occupationally exposed to known human carcinogens.[20] Painters have consistently shown significant excess in lung cancer mortality for both smokers (relative risk of 1.35 (95% CI: 1.21–1.51) and nonsmokers (relative risk of 2.00 (95% CI: 1.09–3.67)).[21] They also have a

CONTACT Ilias G. Kavouras ilias.kavouras@sph.cuny.edu Department of Environmental, Occupational and Geospatial Health Sciences, CUNY Graduate School of Public Health and Health Policy, 55 W. 125 Street, New York, NY 10027

Supplemental data for this article can be accessed at tandfonline.com/uoeh. AIHA and ACGIH members may also access supplementary material at http://oeh.tandfonline.com/.

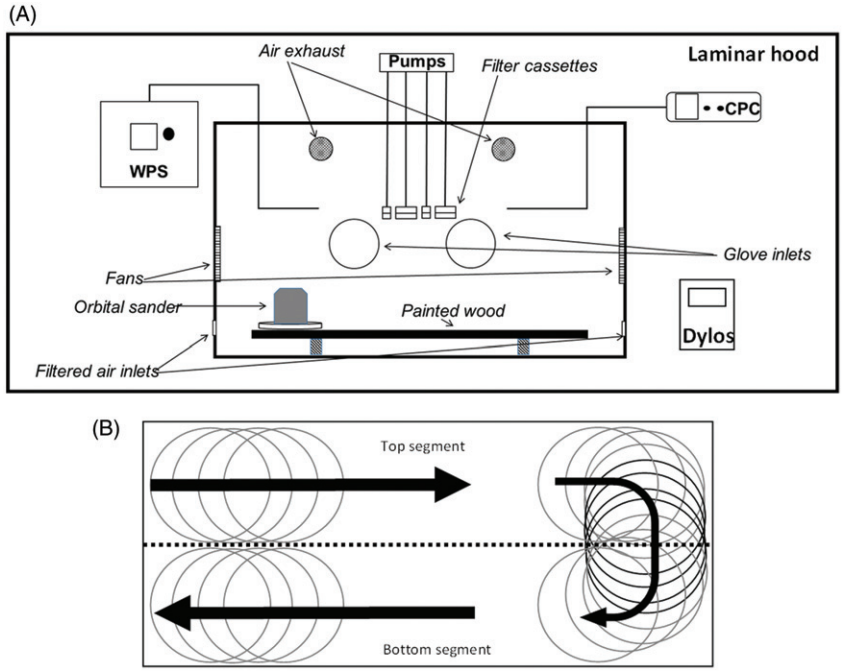

Figure 1. Schematic drawing (not-in-scale) of the Coatings Aerosol REsuspension System (CARES) (A). The painted surface was placed within the chamber and manually abraded with an orbital sander in a predetermined pattern (B). The released dust was analyzed by real-time monitors and collected on appropriate substrates for chemical and morphological analysis.

higher than average incidence rate (235.9 per 10,000 workers; average of 104 per 10,000 workers) for nonfatal occupational injuries/illness and a median of 9 days away from work, with exposures to harmful substances being the dominant nonphysical hazard.[22] Painting is associated with rhinitis symptoms (odds ratio: 2.4, 95% CI: 1.1–5.2), asthma (odds ratio: 4.7, 95% CI: 1.4–16.1) and chronic bronchitis (odds ratio: 2.9, 95% CI: 1.0–8.4) when compared to carpentry work.[23]

The current risk assessment process in occupational health and safety focuses on individual chemicals, which may not be appropriate to address possible health risks of paints with nanoparticles throughout the lifecycle of the product. In paints, nanoparticles form agglomerates with paint polymers; however, the integrity of these agglomerates may be compromised by environmental and mechanical factors resulting in metals and metal oxides dislocation and release over time.[24–27] An important *"end-of-life"* exposure scenario that directly leads to the generation of respirable paint dust is the mechanical abrasion (i.e., sanding) of painted surfaces. Koponen et al.[28] found that sanding dust of wall and wood coated with nano-containing products was dominated by particles in the 100–300 nm size range. Gomez et al.[29] found that 80% of the collected paint dust particles have TiO_2 and Ag nanoparticles based on electron microscopy. These studies raise concerns regarding the potential for exposures to nanoparticles currently incorporated in paints; there is a lack of systematic investigation and understanding of the parameters affecting the release and their physicochemical and morphological properties.

The aims of this study were to: (i) determine the number concentration and size distribution; (ii) characterize the elemental and organic composition; and (iii) assess the presence of TiO_2, in released particles generated by the mechanical abrasion on wood surfaces painted with TiO_2-containing paint for different painting and mechanical abrasion conditions. For this purpose, a coating aerosol generation system has been developed to simulate the realistic generation of paint dust during sanding including commercially available wood surfaces, paints, sanders, and sandpapers typically used by painters in the construction industry. Paint dust samples were collected and their morphology and chemical content were determined by scanning electron microscopy (SEM), attenuated total reflectance Fourier-transformed infrared (ATR-FTIR), and inductively coupled plasma mass spectrometry (ICPMS).

Methods

Paint dust generation

Figure 1A shows the schematic diagram of the major components of the Coatings Aerosol Resuspension

System (CARES). It is composed of a polyvinylchloride glovebox chamber (115 cm [L] × 60 cm [W] × 60 cm [H]) (Lancs Industries, Kirkland, WA) that is installed in laminar-flow ventilation hood (SG603 Model, Baker Co., Sanford, ME). Mechanical abrasion of the painted surface is done manually using an orbital sander. The inlets of the aerosol continuous monitors and integrated samplers are placed on the upper surface of the chamber, approximately 40 cm above the working surface, to better simulate the distance between the wall and a painter's breathing zone. Fans on the side panels of the chamber ensured dispersion of particles. Additional air was introduced through a high-efficiency particulate filter (HEPA) to reduce the presence of background particles. Excess air was vented through filters to the ventilation hood. Particle number concentrations were continuously measured using DC1700 portable particle counters (Dylos Corp., Riverside, CA) inside the ventilation hood to ensure that particle background levels, before, during, and after the experiments were kept low to eliminate potential contamination of paint dust measurements and for safety.

The aerosol size distribution was monitored using a suite of continuous particle sizers and counters that directly measure the aerodynamic diameter (d_a). These include the wide particle spectrometer (WPS) (Model 1000XP, MSP Corp., Shoreview, MN) and the condensation particle counter (CPC) (Model 3771, TSI Inc., Shoreview, MN). The WPS measured particles from 10 nm to 10 μm using differential mobility analyzer coupled with condensation particle counting (DMA/CPC) for particles with $d_a < 0.4\,\mu$m (in 48 channels for 3 sec/channel) and optical light scattering (OLS) for particles with $d_a > 0.4\,\mu$m (in 24 channels concurrently). The particle concentration ranges were up to 20×10^7 part/cm^3 for the DMA/CPC and 500 part/cm^3 for the OLS sensor. The CPC measured the total number of particles with $d_a > 10$ nm. Particles in the sample stream are grown through the condensation of isopropanol vapors and counted using a single-particle-count mode. Paint and wood dust samples were collected on two sets of 13-mm cellulose filters and 47-mm Teflon filters (Pall Corp., Port Washington, NY) at 1.0 and 5.0 L/min flow rate, respectively, for subsequent SEM, ATR-FTIR, and ICPMS analysis. The 13-mm filters were selected to fit on SEM sample holder. The Teflon filters were selected to facilitate gravimetric, elemental, and organic analysis (not shown here).

Painted surface preparation and abrasion

A commercially available latex paint and primer formulation for indoor surfaces was purchased. These paints are typically composed of pigments, fillers, and binders in an aqueous suspension. According to the product's safety datasheet, the paint formulation was composed of water (49.6% w/w), nonvolatile species (49.4% w/w), organic volatiles (0.9% w/w), and 2-amino-2-methyl-1-propanol (0.2% w/w) (CAS #: 124-68-5). It also included TiO_2 (3.2% w/w) (CAS #: 13463-67-7), crystalline silica (0.22% w/w) (CAS #: 14808-60-7), and cristobalite (0.11% w/w) (CAS #: 14464-46-1). Both sides of the wood panels (61.25 cm [L] × 28.75 cm [W]) were coated with two, four, six, and eight paint coatings by using a 5-cm brush with 48-hr waiting periods between coatings. Six to eight replicates were collected for each sampling configuration. Panels were conditioned in a room (20°C and 30% RH) for a week prior to sanding.

For abrasion, a BDERO600 2.4 Amp 5 in (12.7 cm) orbital sander in its complete configuration (including the fitted filter) (Black & Decker, Towson, MD) fitted with Shopsmith 5 in (12.7 cm) aluminum oxide abrasive film discs (sandpaper, hereafter) (Shopsmith, Dayton, OH) was used. The sandpaper grits were 40, 120, and 220 (P_{40}, P_{120} and P_{220}, hereafter) and correspond to "Step 1: Extreme removal", "Step 2: Moderate surface preparation", and "Step 3: Fine scuffing" in the wood preparation and polishing processes. Each wood panel was divided in two segments (Figure 1B). The sander was manually moved on the top segment along its length for 2.5 min, then vertically to the bottom segment and along its path for another 2.5 min. The sanding duration for each segment was selected to match the time required by the WPS to perform two full scans for the entire particle size range (two measurements ×144 sec/measurement +15 sec delay between measurements). A new sandpaper pad was used for each experiment. A set of wood panels underwent the same treatment (handling and sanding, except painting) to characterize the physicochemical and morphological properties of wood dust. All activities were performed by a doctoral research assistant to control reproducibility uncertainties associated with differences in operator's behavior. Breaks were scheduled between tests to perform background tests on instruments and experimental setup and reduce operator's fatigue and ergonomic hazards.

Chemical and morphological analysis

The 47-mm Teflon filters were analyzed by ICP-MS for Al, Si, Ti, Zn, and K at the University of Arkansas at Fayetteville Stable Isotope Laboratory. Samples were digested in concentrated HF/HNO_3 mixtures.

Following digestions, samples were evaporated to dryness and re-dissolved in 2 mL of HNO_3. Prior to analysis, the sample was diluted with ultrapure water and known quantities of internal standards were added. ATR-FTIR spectra of wood dust, paint, and paint dust samples were measured using an ALPHA spectrometer (Bruker Corp., Billerica, MA) equipped with a single reflection diamond ATR. The spectra were recorded in the range of 400–4000 cm^{-1} with a resolution of 2 cm^{-1} over 64 scans. The morphology of paint dust particles was visualized by SEM (Quanta 650 FEG, Eindhoven, the Netherlands) under low-vacuum at an accelerating voltage of 15 kV at the University of Alabama at Birmingham Scanning Electron Microscopy Laboratory. Prior to analysis, the samples were mounted on brass stub and sputtered with Pt. The working distance of samples was set at 10 mm with an accelerating voltage of 5 kV and a diaphragm of 30 μm. Images were taken at 5000× magnification. Elemental compositions were examined using an energy-dispersive X-ray spectroscopy analyzer with 30 mm^2 Silicon Drift spectrometer. Energy dispersive spectroscopy (EDS) analyses were performed at a magnification of 5000×, corresponding to an analyzed surface of 50 μm [w] × 30 μm [h]. It is noteworthy that the d_a measured by the particle sizers described previously refers to the diameter of the spherical particle with a density of 1,000 kg/m^3 and the same settling velocity as the irregular particle, while SEM measurements refers to the actual physical size of the particle.

Calculations

The count median diameter (CMD) and geometric standard deviation (GSD) were computed by plotting the particle number cumulative fraction as a function of particle diameter for each sample. The particle mass concentration (m in $\mu g/m^3$) for thoracic (PM_{10}), fine ($PM_{2.5}$), accumulation-mode ($PM_{1.0}$), and nano-sized ($PM_{0.1}$) particles were computed using the WPS data as follows:

$$PM_x = \left(\sum_{i=1}^{n} \frac{\pi \cdot d_{a,i}^3 \cdot \rho_p \cdot N_i}{6} \right) \cdot 10^9, \qquad (1)$$

where x is the PM fraction ($PM_{0.1}$, $PM_{1.0}$, $PM_{2.5}$, or PM_{10}), $d_{a,i}$ (in m) and N_i (in $part/m^3$) were the mid-point particle aerodynamic diameter and number concentration for i-channel, and ρ_p was the particle density of 1,000 kg/m^3 that is typical for carbon-rich particles. For PM_{10}, all WPS channels were used. The channels with mid-point d_a from 0.01–0.103 μm, to 1.09 μm and 2.29 μM were integrated for $PM_{0.1}$, $PM_{1.0}$, and $PM_{2.5}$ mass estimates. The mean particle CMD, GSD, and number and mass concentrations were computed from all replicates for each test ($n = 6$–8).

Particle number concentrations (PNC) were log-transformed and tested for normality using the Shapiro-Wilk test. The significance of difference in mean PNC values between groups was examined with the nonparametric Mann-Whitney (when two groups where compared) and Kruskal-Wallis (for more than two groups) tests at $\alpha = 0.05$. These tests were followed by Tukey's Honestly Significant Difference test. All analyses were done using SPSS (Version 23) (IBM Analytics, Armonk, NY) and Origin Pro (version 9.1) (OriginLab, Northampton, MA).

Results

Particle concentrations and size distribution

The panel A in Figure 2 illustrates the PNC of wood and paint dust (two paint coatings) generated by the sander for approximately 5 min using different sandpaper grits. The panel B in Figure 2 shows paint dust PNS for multiple paint coatings using the P_{120} sandpaper. The mean (± standard error of the mean) PNC in paint dust varied from 147,000 ± 1,500 $part/cm^3$ for

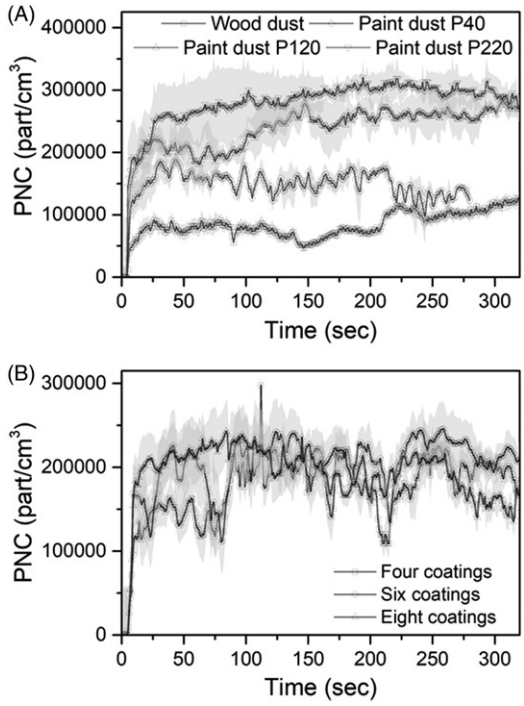

Figure 2. The particle number concentration of (A) wood dust using P_{120} and paint dust with P_{40}, P_{120}, and P_{220} sandpapers and (B) paint dust with P_{120} sandpaper used to remove four, six, and eight coatings, both as measured by the condensation particle counter.

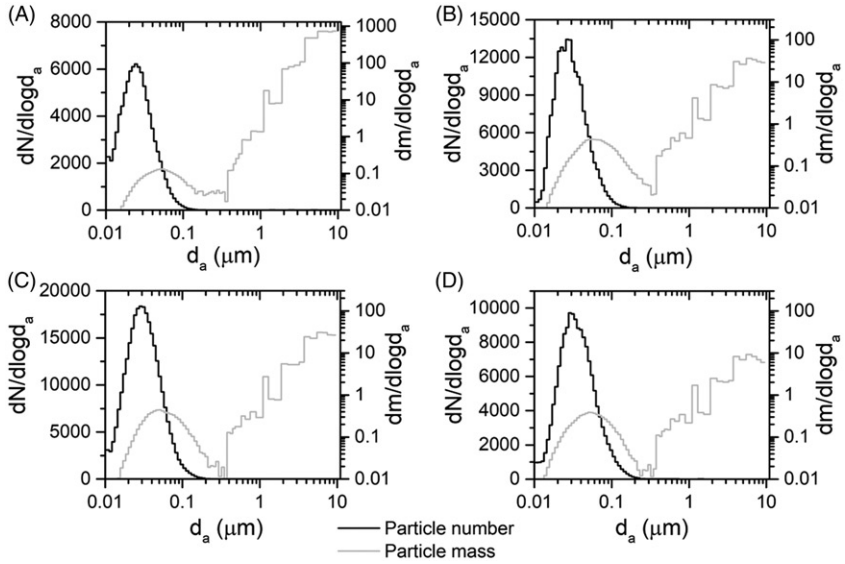

Figure 3. Particle number and mass (in logarithmic scale) size distribution of (A) unpainted wood and paint dust with (B) P_{40}, (C) P_{120}, and (D) P_{220} sandpapers.

the P_{40} sandpaper to 235,000 ± 2,200 part/cm^3 for the P_{120} sandpaper and 278,000 ± 2,300 part/cm^3 for the P_{220} sandpaper. They were consistently higher than the wood dust PNC (83,000 ± 1,100 part/cm^3) using the P_{120} sandpaper (differences were statistically significant at the 95% level).

Paint dust PNC followed a multimodal pattern as the orbital sander moved along the painted surfaces (segment #1 in Figure 2A). The trends were more pronounced for paint dust generated using the P_{40} sandpaper and to a lesser extent for P_{120} and P_{220} sandpapers. Wood dust showed little temporal variability. For paint dust generated using the P_{40} sandpaper, the PNC at the end of this modal cycles were comparable to the PNC measured for wood dust (segment #2 in Figure 2A). It is noteworthy that paint was completely removed using the P_{40} sandpaper and only partially for P_{120} and P_{220} sandpapers were used (see Figure S1 in Supplemental Information).

The PNC of paint dust generated using the P_{120} sandpaper for wood panels with multiple paint coatings (i.e., four, six, and eight) varied from 178,000 ± 2,000 part/cm^3 to 200,000 ± 2,000 part/cm^3) (Figure 2B) (differences were also statistically significant at the 95% level). The multimodal PNC pattern over time was also observed for the multiple paint coatings. Its intensity (i.e., variability between maximum and minimum PNC) decreased as the coating layers increased. Note that paint was also inefficiently removed from panels with multiple coatings (see Figure S2 in Supplemental Information).

Figures 3A–D and 4A–C depict the normalized measured particle number and reconstructed mass

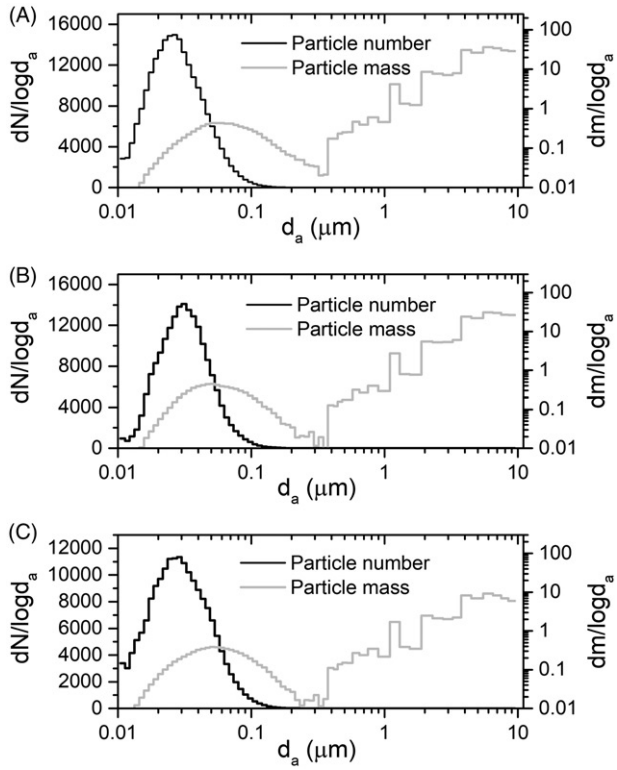

Figure 4. Particle number and mass (in logarithmic scale) size distribution of paint dust using P_{120} sandpaper on (A) four, (B) six, and (C) eight coating layers.

(ca. Eq. (1) for each size range) size distributions of wood dust, paint dust using different sandpapers and for variable paint coatings. A one-mode distribution with maxima in the nano size range ($d_a < 100$ nm) was observed for paint dust particle number generated by different sandpapers and multiple paint coatings. The size distribution of particle mass reached a

TABLE 1. Paint dust aerosol size characteristics and mass concentrations (mean ± standard error).

	Wood dust	Paint dust					
Sandpaper	P_{120}	P_{40}	P_{120}	P_{220}	P_{120}	P_{120}	P_{120}
Paint coatings	—	2	2	2	4	6	8
CMD (nm)	31 ± 5.4	38.4 ± 1.6	39.4 ± 2.7	35.6 ± 2.2	28.5 ± 1.9	35.5 ± 2.4	27.2 ± 1.5
GSD	2.8 ± 0.1	2.4 ± 0.1	2.2 ± 0.1	2.2 ± 0.1	2.4 ± 0.1	2.2 ± 0.1	2.3 ± 0.1
MMD (nm)	679 ± 122	356 ± 41	269 ± 41	230 ± 40	284 ± 34	229 ± 38	284 ± 30
d_{mm} (nm)	1,135 ± 204	515 ± 60	370 ± 56	314 ± 54	416 ± 50	313 ± 53	308 ± 42
Particle mass[a] ($\mu g/m^3$)							
TSP	16,222 ± 1,074	5,582 ± 1,386	1,113 ± 442	329 ± 35	864 ± 503	729 ± 428	229 ± 44
$PM_{0.1}$	3 ± 1	7 ± 2	17 ± 3	12 ± 3	9 ± 1	9 ± 1	8 ± 1
PM_1	16 ± 1	25 ± 2	36 ± 5	32 ± 15	20 ± 3	17 ± 2	15 ± 1
$PM_{2.5}$	359 ± 37	269 ± 65	94 ± 21	49 ± 15	72 ± 29	50 ± 20	31 ± 3

[a]Assuming spherical particles with a density of 1,000 kg/m^3

maximum in the coarse particle range ($d_a > 2.5\ \mu m$). For paint dust generated by P_{120}, P_{220} and to a lesser extent for paint dust from multiple paint coatings, a second mode in particle mass distribution was observed in the accumulation mode ($d_a < 1\ \mu m$) (see arrows in Figures 3C–D and 4B–C).

Table 1 presents the mean (± standard error) of the CMD, GSD and reconstructed PM_{10}, $PM_{2.5}$, $PM_{1.0}$, and $PM_{0.1}$ mass concentrations (ca. using Eq. (1)). Paint dust was comprised of nano-sized particles with a CMD of 35.6–39.4 (38.4 ± 1.6 nm for P_{40}, 39.4 ± 2.7 nm for P_{120}, and 35.6 ± 2.2 nm for P_{220}). The CMD of wood dust (with P_{120} sandpaper) was comparable (31.0 ± 5.4 nm). The GSDs of paint dust particles were also similar for paint dust generated with the different sandpapers (2.4 ± 0.1 for P_{40} and 2.2 ± 0.1 for P_{120} and P_{220}), while a slightly higher GSD was computed for wood dust (2.8 ± 0.1) suggesting that larger particles may be present in wood dust. This was in agreement with the higher mass median diameter (MMD) (679 ± nm) and diameter of the mean mass (d_{mm}) (1,135 ± 204 nm) of wood dust as compared to those computed for paint dusts (MMD: 229 ± 38 to 356 ± 41 nm; d_{mm}: 308 ± 42 to 515 ± 60 nm). Comparable CMD (from 27.2 ± 1.5 to 35.5 ± 2.4) and GSD (from 2.2 ± 0.1 to 2.4 ± 0.1) (Table 1) values were calculated for paint dust generated using the P_{120} sandpaper on wood surfaces covered with multiple paint coatings.

Assuming spherical particles with density of $\rho_p = 1{,}000\ kg/m^3$ (i.e., typical for carbon–rich aerosol), the reconstructed mean (± standard error) PM_{10} mass concentration of wood dust was 16.2 mg/m^3. It was substantially higher than the reconstructed PM_{10} mass concentration for paint dust using the three sandpapers. The paint dust PM_{10} concentration increased from 329 ± 35 to 5,582 ± 1,386 $\mu g/m^3$ as the sandpaper grit size decreased (from ultrafine to coarse sandpapers). For wood dust, the vast majority of PM_{10} mass were coarse particles (~98%), and only one-thousandth (or 16 ± 1 $\mu g/m^3$) was associated with the finer particles ($PM_{1.0}$) and one tenth of that was in the nano size ($PM_{0.1}$) range (3 ± 1 $\mu g/m^3$).

Approximately 5–15% of paint dust PM_{10} was associated with the respirable fraction ($PM_{2.5}$) (269 ± 65 $\mu g/m^3$ for P_{40}, 94 ± 21 $\mu g/m^3$ for P_{120}, and 49 ± 15 $\mu g/m^3$ for P_{220}). The $PM_{1.0}$ fractions accounted for 10%, 30%, and 55% of $PM_{2.5}$ paint dust generated with P_{40}, P_{120}, and P_{220} sandpapers, with 25-50% of them being in the nano size range, resulting in $PM_{0.1}$ mass concentrations as high as 17 ± 3 $\mu g/m^3$. The paint dust PM_{10} mass concentrations decreased from 869 ± 503 $\mu g/m^3$ to 229 ± 44 $\mu g/m^3$ as the number of applied paint coatings increased from four to eight, albeit around 10% was associated with the fine fraction. The $PM_{1.0}$ fraction account for 25–50% of $PM_{2.5}$, with more than 50% of $PM_{1.0}$ particles being in the $PM_{0.1}$ size range.

Paint dust composition

Chemical analysis

The ATR-FTIR absorbance spectra of wood and paint are depicted in Figure 5A. The spectrum of wood dust demonstrated unique absorption bands including stretching O—H in-plane absorption bands in the 3200–3700 cm^{-1} typical in cellulose and polysaccharides. Other major absorption bands were attributed as follows: 2800–3000 cm^{-1} to C—H stretching, 1510 cm^{-1} to C=C stretching of the aromatic ring of lignin, 1465 cm^{-1} to C—H deformation in lignin, 1375 cm^{-1} to C—H deformation in polysaccharides, 1335 cm^{-1} to bending in-plane O—H, 1240 cm^{-1} to C—O stretch in lignin and broad band in 1024 cm^{-1} to C—O stretch in C—O—C cellulosic bridges.

The main absorption bands observed in the ATR-FTIR spectrum of paint were: 2800–3000 cm^{-1} (stretching vibration of the —CH_2— group), 1730 cm^{-1} (stretching of the C=O group), 1450 cm^{-1}, 1385 cm^{-1} (stretching of CH_3 groups), 1240 cm^{-1}

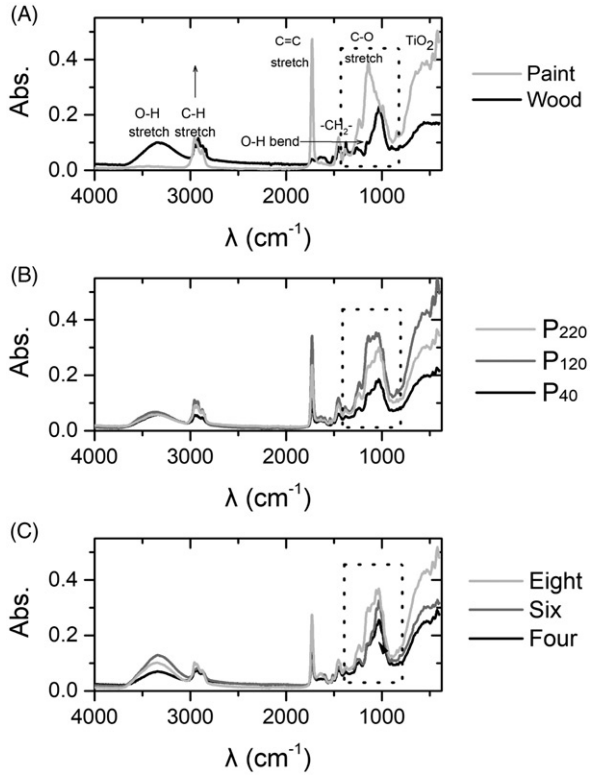

Figure 5. ATR-FTIR spectra of (A) wood dust and paint, (B) paint dust with P_{40}, P_{120}, and P_{220} sandpapers, and (C) four, six, and eight coatings.

(stretching of =C—H groups), 1140 cm^{-1} (stretching of the C—O group), and 840 cm^{-1} (bending vibration of the aromatic C—H group). The broad bands in 400–650 cm^{-1} region were assigned to TiO_2.

Figures 5B and C show the ATR-FTIR spectra of paint dust generated with variable sandpapers and multiple coatings, respectively. Clear similarities among paint dust, paint and wood spectra can be detected, reflecting the presence of both paint and wood species in paint dust. All paint dust samples retained the absorption bands in the 400–650 cm^{-1} region, previously attributed to TiO_2. Per Beer-Lambert Law, the absorption is proportional to the concentration; thus, more TiO_2 may be associated with paint dust generated with P_{120}/P_{220} sandpapers as compared to P_{40} sandpaper, and for paint dust generated from six and eight coatings compared to four coatings. The relative abundance of paint and wood particles may be derived from the spectral profile in the 800–1300 cm^{-1} region (dotted rectangular in Figures 5A–C) that includes C—O absorption bands for wood dust (cellulosic and lignin) and paint dust (oil-based binders). The relative contribution of paint species in paint dust increased as the sandpaper grit changed from P_{40}–P_{220} and the number of coatings increased. The prevalence of wood species also

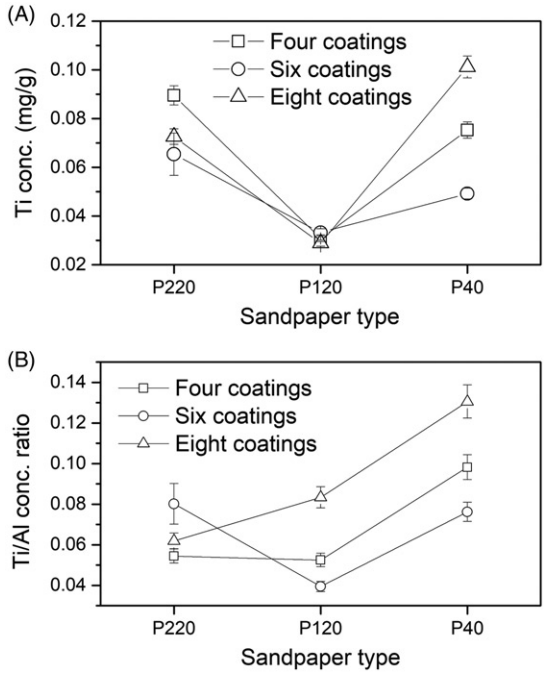

Figure 6. Composition of paint dust generated by sanding wood boards coated with multiple paint layers with different sandpapers, for (A) particulate Ti concentration and (B) Ti to Al concentration ratios.

increased for different sandpapers but remained relatively unchanged for multiple coatings.

Figures 6A–B show Ti concentrations in paint dust (in ng/mg of paint dust particles) and the Ti-to-Al ratios generated using three sandpaper types for multiple paint coatings measured by ICPMS. The measured levels of Ti, Al, Si, K, and Zn are presented in Table S1. Paint dust Ti concentrations using the P_{120} sandpaper were comparable for all coatings (from 29–33 ng/mg of particles) but lower than those measured using the P_{40} (from 49–101 ng/mg of particles) and P_{220} (from 73–90 ng/mg of particles) sandpapers. Overall, Ti in the form of TiO_2, accounted for 0.01–0.02% by weight of total particle mass. Note that no size selective inlet was used, therefore the total suspended particulate (TSP) aerosol including large wood dust particles were collected. Assuming that TiO_2 particles may be present in the nano size range and that $PM_{0.1}$ particles accounted for approximately 1% of TSP by mass (Table 1), the relative abundance of TiO_2 may increase up to 2% by mass.

Aluminum (Al) was present in paint (see Figure 8 below) but can also be released from sandpaper. The Ti/Al ratio was used to assess the potential effect of sandpaper particles for different sandpapers and paint coatings. For wood panels with the same paint coatings (similar quantities of paint TiO_2), higher Ti/Al values indicated an enrichment of TiO_2 as compared

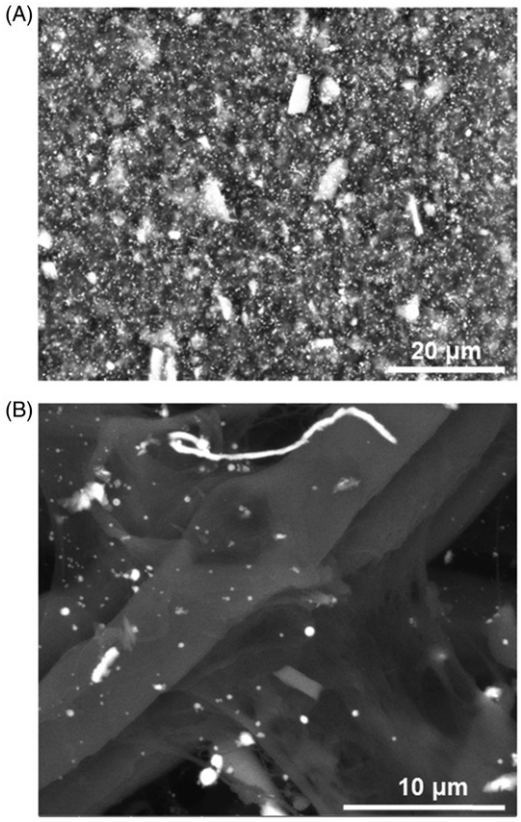

Figure 7. Backscattering SEM image (5,000x magnification) of (A) paint and (B) paint dust using P_{120} sandpaper and two paint coatings.

to larger Al-containing particles in paint or sandpaper. In most of the experiments, the Ti/Al increased for coarse sandpapers suggesting the enhanced presence of paint particles as compared to those potentially released from sandpaper. In all cases, Al and Si concentrations added less than 1% to paint dust particle mass.

Morphological analysis

Figure 7 depicts the SEM backscattering images of paint and paint dust generated by P_{120} with two coatings. SEM images of paint dust generated with different sandpapers and coatings are included in Supplemental Information (see Figures S3 and S4 in Supplemental Information). In backscattering SEM, carbon-based materials are projected in dark colors whereas elements are bright. The painted surface is characterized by a rather uniform distribution of white spots that may be attributed to metal oxides. Released particles also contained TiO_2 nanomaterials in various shapes (spherical, amorphous) in the nanosize range (Figure 7B and Figure S5 in Supplemental Information). Larger fiber agglomerates were in the submicron range.

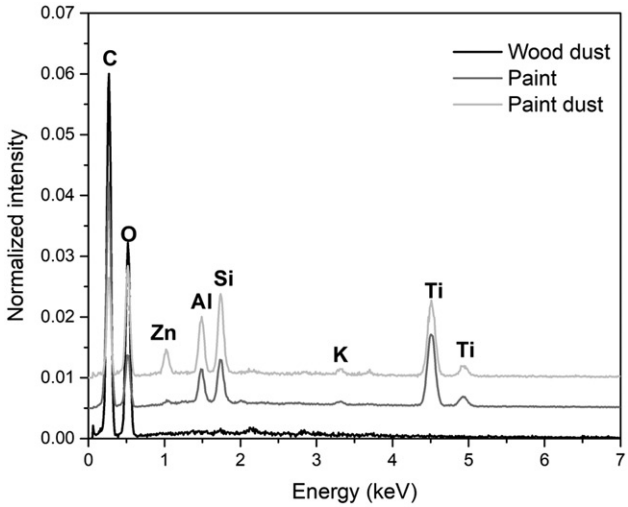

Figure 8. Typical SEM EDS spectra of individual particles in wood, paint and paint dust (P_{120} sandpaper, and two coatings).

Figure 8 shows typical SEM-EDS spectra obtained from wood, paint and paint dust. Wood dust was entirely composed of C and O (ratio of 2:1). This is comparable to the compositional characteristics of wood, that is comprised of 80% of cellulose (represented as CH_2O, C:O = 1) and 20% lignin (represented as $C_{10}H_{13}O_4$, C:O = 5:2). No metals were observed in wood dust. In addition to C and O (ratios of 4:1 for paint and 1:1 for paint dust), paint and paint dust also comprised of Ti, Al, and Si. Traces of Zn and K were observed in paint dust. The quantity of Ti was comparable in paint and paint dust (23 and 24%). The relative abundance of Si and Al increased from 12% and 7% in paint to 19% and 14% in paint dust, respectively. That may be suggestive of minor quantities of Al and Si particles released from the sandpaper. Note that C may also be associated with the filter material (cellulose).

Discussion

The PNCs of dust generated from bare and painted wood surfaces with multiple paint coatings using different sandpapers have been monitored. Paint dust PNC was up to three times higher than wood dust PNC due to differences on wood and paint surface properties affecting particle generation.[30] Wood contains long fibers made of cellulose and lignin ranging from 30–300 μm in diameter and 10 μm–4 mm in length.[31] On the other hand, painted surfaces are composed of single particles associated with pigments, filler particles in agglomerates with the polymeric binder, and other additives (e.g., thickeners, dispersants, and defoamers) to achieve stability and

application consistency. The type, size, and quantity of pigments varied (TiO_2 for white and high opacity paint), but typical pigment particle sizes did not exceed 250 nm in diameter. Larger agglomerates may be in the submicron size range.[32] Paint dust PNC increased for finer sandpaper, which is consistent with the potential of particle in finer sandpapers to make chiseled scratches and dislocate smaller pieces of paint materials. On the other hand, coarse sandpaper has the capacity to remove larger quantities of material by generating larger particles, which was consistent with the particle size measurements and particle mass calculations. Another potential mechanism, albeit of minor importance for engineered metal-oxides nanoparticles, is the volatilization of paint organic polymers because of the heat developed on the surface by friction, and subsequent particle formation through condensation.

Previous studies have also found that engineered nanoparticles in wood sealants and coatings to protect against water and UV damage on plywood and hardwood panels may be released as agglomerates by mechanical abrasion.[33,34] Those studies, however, found no significant differences in PNC between coated and uncoated surfaces. This may be due to differences on the thickness of coating materials (paint vs. sealants) and the type of wood panel. Plywood is made of thin wood layers patched, graded, glued, and baked together, compromising the integrity/length of wood fibers, which may result in the generation of more nano-sized particles during sanding. It has been previously reported that nano-sized particles may be generated by the orbital sander.[28] In this study, both measured paint and wood dust concentrations include sander-generated nanoparticles. As a result, even if all nano-sized particles in wood dust were due to the sander, they could only account for up to 30% of paint dust nanoparticles. Previous studies suggested that submicron particles may also be generated by the degradation of sandpaper, as indicated by the presence of Si-Al particles.[28] Note that the average sandpaper particle diameters for P_{220}, P_{120}, and P_{40} sandpapers were 68, 115, and 425 μm, respectively.[33] In this study, SEM/EDS analysis indicated the presence of Al and Si in paint and paint dust but not in wood dust generated using the same sandpapers. Elemental analysis by ICPMS showed that Al and Si particles accounted for less than 1% of particle mass. The coarse sandpapers may have less Al particles than finer grits.

Paint application of new wood surfaces in residencies and buildings typically includes one layer of primer, ultrafine sanding to smooth the wood surface, and two subsequent layers of paint. However, over time, more layers of paint may be applied without sanding. This may result in the accumulation of paint components including nanoparticles. No significant differences in PNC from surfaces coated with multiple paint layers were observed indicating that particle release rates under the same conditions (i.e., sandpaper and sanding time) were comparable. However, more nano-sized particles may be eventually re-suspended from multiple painted surfaces because more time would be required to remove the accumulated paint effectively.

Nano-sized range particles were predominantly generated during abrasion of bare and painted wood surfaces. The CMD did not vary substantially (differences not significant at the 95%) for wood and paint dust generated by different sandpaper grits. On the other hand, GSD differences among wood and paint dusts were statistically significant at the 95% level indicating that generation of nano-sized particles is favorable in painted surfaces. Wood dust was comprised of more coarse particles (with $d_a > 2.5\,\mu$m) and less nano-sized range particles (with $d_a < 100$ nm) compared to those measured for paint dust. As a result, more than 98% of wood particles by mass were not respirable. In comparison, on average 9.5% of paint dust particles by mass were respirable (from 1.8–14.9% for different sandpapers and coatings), with 20% of the respirable fraction being in the nano-size range (from 2.6–25.8% for different sandpapers and coatings). It is noteworthy that instantaneous particle size changes may not be entirely captured because of the WPS measurement method in which particle number concentration for different sizes is measured sequentially. This uncertainty may be more important as the sander moved on smoothed surfaces; however, the total PNC measured by WPS and average PNC measured by CPC for the same time period were comparable (percent of coefficient of variance (%CV) of less than 7%), indicating that there were no major particle size misclassification during the measurement period.

The types of the abraded surface and sandpaper modified the particle size range and their quantity (by number and mass concentration) but not the central tendency indicators (CMD). The production of more nano-sized paint particles may be related to the force energy required to break agglomerates of pigments, filler particles, and other additives in paints as compared to large cellulosic/lignin fibers in wood. When paint is applied, its ingredients may adhere to the

wood surface through mechanical interlocking, diffusion, adsorption, and surface reaction and electrostatic interactions. More paint on wood surfaces (i.e., from painting over existing paints) may result in the release of more nano-sized particles by mechanical abrasion because additional time would be required to remove all paint layers from the wood surface efficiently.

The release of paint materials included TiO_2 nanoparticles have been further confirmed by ATR-FTIR, SEM microscopy, and ICPMS spectroscopy. Paint components accounted for the majority of organic and inorganic components in paint dust particles (no IR absorbance assigned to inorganic species was observed in wood dust). TiO_2 nanoparticles are found to be encapsulated or on the surface of nano-sized paint particles and individually in different shapes and sizes mostly in the nano range. The relative abundance of TiO_2 on individual paint dust particles (as quantified by EDS detector in SEM) was comparable to that measured in paint. Compared to particle mass, TiO_2 nanoparticles accounted for 0.01–0.02% of TSP mass and up to 1–2% in the nano-size range. Albeit lower than the recommended NIOSH airborne exposure limit of 0.3 mg/m^3, the risk for adverse health effects through the inhalation of nano-sized particles containing engineered nanoscale TiO_2 may not be discounted.

Previous studies showed that the toxicity of TiO_2 nanoparticles following 24-hr of exposure may be negligible compared to the toxicity of pristine TiO_2; however, the long-term effect (48, 76, or 120 hr after exposure) was not examined.[34] Donaldson et al.[35] demonstrated lung responses and distribution to other organs after 2–28 days following month-long exposures, indicating the persistence of TiO_2 nanoparticles. Encapsulated nanoparticles in agglomerates of water-based paint polymers in the submicron range ($d_a < 1\ \mu m$) can still penetrate into the alveolar region and, upon decomposition, dissolution and/or uptake of the water-soluble polymer, they may be released intact in the lung or distributed in other organs maintaining their enhanced toxicity. The timing of TiO_2 release by dissolution of the paint polymers may also be important since nanoparticles can also translocate into the blood stream affecting other organs.

Currently, there are exposure limits for specific components integrated in paints (lead, chromium (VI)), but there is no exposure limit for paint dust or newer additives. The estimated total particle mass concentrations in this study were lower than the exposure threshold for wood dust (15 mg/m^3), even though the wood dust TSP mass concentration exceeded the exposure threshold. However, the abundance of nano size particles is particularly worrisome (as high as 17 $\mu g/m^3$) as their estimated surface area may range from 4–23 cm^2/m^3. It is noteworthy that the estimated particle mass exposures from this study do not represent actual personal exposures because a smaller chamber (~0.5 m^3) was smaller than a typical size (20–30 m^3), which may overestimate exposure, albeit the ventilation hood was operating at 800 m^3/hr flow rate leading to high air exchange rates in the CARES system (may dilute/underestimate exposure estimates). It has been previously shown doses of nano size particles substantially lower than those measured in this study may induce severe pulmonary toxicity and significant pulmonary inflammation and cytotoxicity potencies for TiO_2 doses as low as 0.0125 cm^2/cm^3.[36–38]

Conclusions

Metal and metal oxides nanoparticles have been integrated in paints and other construction materials because of their ability to improve their performance. Exposures to nanoparticles may be minimal assuming proper handling and use of the products, but little is known about the potential for exposures to nanoparticles at the end of paint's lifecycle, which includes the removal of paint from surfaces by sanding. Our analysis clearly demonstrated the potential for the release of elevated particle concentrations. The majority of these particles were in the nano-size range accounting for up to 50% of respirable particulate matter. The nano-size particle number concentrations increased for finer sandpaper grits and more paint coatings; albeit lower particle mass concentrations were estimated. Chemical and morphological analysis determined that paint dust particles were comprised of a combination of paint and wood species including TiO_2 nanoparticles embedded in paint. These nanoparticles were found predominantly attached on the edge or inside particle agglomerates, albeit still in the nano-size range, therefore enabling the potential for penetration of nanoparticles containing nanoparticles in the lung alveoli and translocation into the blood.

The paint dust exposure generation system and use of commercially available equipment and supplies afforded the capability to simulate typical occupational conditions in a reproducible and traceable manner. Because of its modality, the generation system may be utilized to investigate a wide spectrum of exposure scenarios including paint and coating application by spraying. These findings call for further research into

the release of nanoparticle-embedded paint dust particles including the effect of the type and quantity of nanoparticles and the effect of weatherization. There is previous evidence that the structural integrity of paint deteriorates over time and that nanoparticles may be released into the environment. Furthermore, *in vitro* and *in vivo* toxicological studies may provide significant insights on the biological effects of paint dust and the role of organic polymers and nanoparticles.

Disclaimer

No potential conflict of interest was reported by the author(s).

Funding

The study was partially supported by the NIOSH funded Deep South Center for Occupational Health and Safety Education and Research Center (Award #: T42OH008436). The findings and conclusions in this report are those of the authors and do not necessarily represent the views of the National Institute for Occupational Safety and Health.

ORCID

Ilias G. Kavouras http://orcid.org/0000-0003-0342-5306

References

[1] **Allen, N.S., M. Edge, A. Ortega, et al:** Degradation and stabilization of polymers and coatings: Nano versus pigmentary titania particles. *Polym. Degrad. Stab.* 85:927–946 (2004).

[2] **Carp, O., C. L. Huisman, and A. Reller:** Photoinduced reactivity of titanium dioxide. *Prog. Solid State Chem.* 32:33–177 (2004).

[3] **Sharma, V.K., R. A. Yngard, and Y. Lin:** Silver nanoparticles: Green synthesis and their antimicrobial activities. *Adv. Colloid Interface.* 145:83–96 (2009).

[4] **Gladis, F., A. Eggert, U. Karsten, and R. Schumann:** Prevention of biofilm growth on man-made surfaces: Evaluation of antialgal activity of two biocides and photocatalytic nanoparticles. *Biofouling.* 26:89–101 (2010).

[5] **Dallas, P., V. K. Sharma, and R. Zboril:** Silver polymeric nanocomposites as advanced antimicrobial agents: Classification, synthetic paths, applications, and perspectives. *Adv. Colloid Interface.* 166:119–135 (2011).

[6] **Holtz, R.D., B.A. Lima, A.G. Souza Filho, M. Brocchi M, and O.L. Alves:** Nanostructured silver vanadate as a promising antibacterial additive to water-based paints. *Nanomed. Nanotechnol.* 8:935–940 (2012).

[7] **Hanus, M.J., and A.T. Harris:** Nanotechnology innovations for the construction industry. *Prog. Mater. Sci.* 58:1056–1102 (2013).

[8] **Schmid, K., and M. Riediker:** Use of nanoparticles in Swiss industry: A targeted survey. *Environ. Sci. Technol.* 42*(7)*:2253–2260 (2008).

[9] **Hoet. P.H.M., I. Bruske-Hohlfeld, and O.V. Salata:** Nanoparticles—Known and unknown health risks. *J Nanobiotechnol.* 2:12–27 (2004).

[10] **Oberdörster, G., E. Oberdörster, and J. Oberdörster:** Nanotoxicology: An emerging discipline evolving from studies of ultrafine particles. *Environ. Health Perspect.* 113:823–839 (2005).

[11] **Liu, J., H.L. Wong, J. Moselhy, B. Bowen, X.Y. Wu, and M.R. Johnston:** Targeting colloidal particulates to thoracic lymph nodes. *Lung Cancer.* 51:377–386 (2006).

[12] **Oberdorster, G., Z. Sharp, V. Atudorei, et al:** Translocation of inhaled ultrafine particles to the brain. *Inhal. Toxicol.* 16:437–445 (2004).

[13] **Semmler, M., J. Seitz, P. Mayer, et al:** Long-term clearance kinetics of inhaled ultrafine insoluble iridium particles from the rat lung, including transient translocation into secondary organs. *Inhal. Toxicol.* 16:453–459 (2004).

[14] **Dasenbrock, C., L. Peters, O. Creutzenberg, and U. Heinrich:** The carcinogenic potency of carbon particles with and without PAH after repeated intratracheal administration in the rat. *Toxicol. Lett.* 88:15–21 (1996).

[15] **Driscoll, K.E., J.M. Carter, B.W. Howard, et al:** Pulmonary inflammation, chemokine, and mutagenic responses in rats after subchronic inhalation of carbon black. *Toxicol. Appl. Pharmacol.* 136:327–380 (1996).

[16] **Shwe, T.T.W., S. Yamamoto, M. Kakeyama, T. Kobayashi, and H. Fujimaki:** Effect of intratracheally instillation of ultrafine carbon black on proinflammatory cytokine and chemokine release and mRNA expression in lung and lymph nodes of mice. *Toxicol. Appl. Pharmacol.* 209:51–61 (2005).

[17] **Nemmar, A., P.H. Hoet, B. Vanquickenborne, et al:** Passage of inhaled particles into the blood circulation in humans. *Circulation.* 105:411–414 (2002).

[18] **Liu, G., P. Mena, P.R.L. Harris, R.K. Rolston, G. Perry G, and M.A. Smith:** Nanoparticle iron chelators: A new therapeutic approach in Alzheimer disease and other neurologic disorders associated with trace metal imbalance. *Neurosci. Lett.* 406:189–193 (2006).

[19] **U.S. Department of Labor:** *Occupational Outlook Handbook, 2016–17 Edition, Painters, Construction and Maintenance.* Bureau of Labor Statistics. Available at https://www.bls.gov/ooh/construction-and-extraction/painters-construction-and-maintenance.htm (accessed June 13, 2017).

[20] **IARC:** Painting, firefighting, and shiftwork. *IARC Monogr. Eval. Carcinog. Risks Hum. 98*:1–804 (2010).

[21] **Guha, N., F. Merletti, N.K. Steenland, A. Altieri, V. Cogliano, and K. Straif:** Lung cancer risk in painters: A meta-analysis. *Environ. Health Perspect.* 118:303–312 (2010).

[22] **U.S. Department of Labor:** *Survey of Occupational Injuries and Illnesses*, Tables 3, 7 and 8. Bureau of Labor Statistics, November 2016. Available at https://www.bls.gov/news.release/archives/osh2_11102016.pdf (accessed June 13, 2017).

[23] **Kaukiainen, A., R. Martikainen, R. Riala, K. Reijula, and L. Tammilehto:** Work tasks, chemical exposure and respiratory health in construction painting. *Am. J. Ind. Med.* 51:1–8 (2008).

[24] **Kaegi, R., B. Sinnet, S. Zuleeg, et al:** Release of silver nanoparticles from outdoor facades. *Environ. Pollut.* 158:2900–2905 (2010).

[25] **Al-Kattan, A., A. Wichser, R. Vonbank, et al:** Release of TiO_2 from paints containing pigment-TiO_2 or nano-TiO_2 by weathering. *Environ. Sci. Process Impacts.* 15:2186–2193 (2013).

[26] **Künniger, T., A.C. Gerecke, A. Ulrich, et al:** Release and environmental impact of silver nanoparticles and conventional organic biocides from coated wooden facades. *Environ. Poll.* 184:464–471 (2014).

[27] **Fiorentino, B., L. Golanski, A. Guiot, J.-F. Damlencourt, and D. Boutry:** Influence of paints formulations on nanoparticles release during their life cycle. *J. Nanopart. Res.* 17:149 (2015).

[28] **Koponen, I.M., K.A. Jensen, and T. Schneider:** Comparison of dust released from sanding conventional and nanoparticle-doped wall and wood coatings. *J. Exp. Sci. Environ. Epidem.* 21:408–418 (2011).

[29] **Gomez, V., M. Levin, E.T. Saber, et al:** Comparison of dust release from epoxy and paint nanocomposites and conventional products during sanding and sawing. *Ann. Occup. Hyg.* 58:983–994 (2014).

[30] **Gohler, D., M. Stinntz, L. Hillemann, and M. Vorbau:** Characterization of nanoparticle release from surface coatings by the simulation of a sanding process. *Ann. Occup. Hyg.* 54(6):615–624 (2010).

[31] **U.S. Department of Agriculture:** *Wood Handbook: Wood as an Engineering Material* (General Technical Report FPL-GTR-113). Forest Products Laboratory, Madison, WI, March 1999.

[32] **Jiang, S., A. Van Dyk, A. Maurice, et al:** Design colloidal particle morphology and self-assembly for coating applications. *Chem. Soc. Rev.* 46:3792–3807 (2017).

[33] **Cooper, M.R., G.H. West, L.G. Burrelli, et al:** Inhalation exposure during spray application and subsequent exposure of a wood sealant containing zinc oxide nanoparticles. *J. Occup. Environ. Hyg. 14*:510–522 (2017).

[34] **Fransman, W., C. Bekker, P. Tromp, and W.B. Duis:** Potential release of manufactured nano objects during sanding of nano-coated wood surfaces. *Ann. Occup. Hyg.* 60:875–884 (2016).

[35] **Federation of European Producers of Abrasives:** *Grain standards.* Grains of fused aluminum oxide, silicon carbide and other abrasive materials for coated abrasives: Macrogrits P12 to P220 FEPA. 43-1, 2006.

[36] **Saber, A.T., I.K. Koponen, K.A. Jensen, et al:** Inflammatory and genotoxic effects of sanding dust generated from nanoparticle-containing paints and lacquers. *Nanotoxicol.* 6*(7)*:776–788 (2011).

[37] **Donaldson, K., V. Stone, A. Clouter, L. Renwick, and W. MacNee:** Ultrafine particles. *Occup. Environ. Med.* 58:211–216 (2001).

[38] **Smulders, S., K. Luyts, G. Bradants, et al:** Toxicity of nanoparticles embedded in paints compared with pristine nanoparticles in mice. *Toxicol. Sci.* 141*(1)*:132–140 (2014).